International Journal of Nanomedicine

Dovepress
open access to scientific and medical research

Open Access Full Text Article

ORIGINAL RESEARCH

Short duration cancer treatment: inspired by a fast bio-resorbable smart nano-fiber device containing NIR lethal polydopamine nanospheres for effective chemo–photothermal cancer therapy

This article was published in the following Dove Press journal:
International Journal of Nanomedicine

International Journal of Nanomedicine downloaded from https://www.dovepress.com/ by 43.243.61.32 on 17-Oct-2018
For personal use only.

Francis O Obiweluozor,[1,2,*] Gladys A Emechebe,[3,*] Arjun Prasad Tiwari,[3] Ju Yeon Kim,[1] Chan Hee Park,[1,3] Cheol Sang Kim[1,3]

[1]Division of Mechanical Design Engineering, Chonbuk National University, Jeonju City, Republic of Korea; [2]Department of Chemical Engineering, Enugu State University of Science and Technology, Enugu State, Nigeria; [3]Department of Bionanosystem Engineering Graduate School, Chonbuk National University, Jeonju City, Republic of Korea

*These authors contributed equally to this work

Background: The objective of this study was to evaluate the efficacy of a combination of Photothermal therapy (PTT) and chemotherapy in a single nano-fiber platform containing lethal polydopamine nano-pheres (PD NPs) for annihilation of CT 26 cancer cells.

Method: Polydioxanone (PDO) nano-fiber containing PD and bortezomib (BTZ) was fabricated via electrospinning method. The content of BTZ and PD after optimization was 7% and 2.5% respectively with respect to PDO weight. PD NPs have absorption band in near-infrared (NIR) with resultant rapid heating capable of inducing cancer cell death. The samples was divided into three groups – PDO, PDO+PD, and PDO+PD-BTZ for analysis.

Results: In combined treatment, PDO nano-fiber alone could not inhibit cancer cell growth as it neither contain PD or BTZ. However, PDO+PD fiber showed a cell viability of approximately 20% after 72 hr of treatment indicating minimal killing via hyperthermia. In the case of PDO composite fiber containing BTZ, the effect of NIR irradiation reduced the viability of cancer cells down to around 5% after 72 h showing the efficiency of combination therapy on cancer cells elimination. However, due to higher photothermal conversion that may negatively affect normal cells above 46°C, we have employed 1 s "OFF" and 2 s "ON" after initial 9 s continuous irradiation to maintain the temperature between 42 and 46°C over 3 mins of treatment using 2 W/cm^2; 808 nm laser which resulted to similar cell death.

Conclusion: In this study, combination of PTT and chemotherapy treatment on CT 26 colon cancer cells within 3 min resulted in effective cell death in contrast to single treatment of either PTT and chemotherapy alone. Our results suggest that this nano-fiber device with efficient heating and remote control drug delivery system can be useful and convenient in the future clinical application for localized cancer therapy.

Keywords: electrospinning, polydopamine nanospheres, chemotherapy, photothermal therapy, electrospun nano-fiber, Bortezomib, local treatment, combination cancer therapy

Introduction

We have reached a point of an urgent need for effective therapeutic approach to cancer diagnosis due to its complexity and wide variation (different types). Although over the past decade, numerous strategies have been developed to treat cancer which is among the leading cause of death in this 21st century, an alternative approach to systemic chemotherapy to treat unresectable tumors and for the prevention of postoperative occurrence such as local treatment has attracted researchers due to its ability to maximize drug concentration toward the targeting site and lower systemic toxicity.[1,2] Currently, numerous researchers are focused on local delivery systems such as hydrogels, wafers, and drug-loaded

Correspondence: Cheol Sang Kim
Department of Bionanosystem Engineering Graduate School, Chonbuk National University, Jeonju City 54896, Republic of Korea
Tel +82 63 270 4284
Fax +82 63 270 2460
Email chskim@jbnu.ac.kr

Chan Hee Park
Chonbuk National University, Engineering Building 9, Unit 413, Baekjedaero 567, Jeonju City 54896, Republic of Korea
Email biochan@jbnu.ac.kr

submit your manuscript | www.dovepress.com
Dovepress
http://dx.doi.org/10.2147/IJN.S180970

© 2018 Obiweluozor et al. This work is published and licensed by Dove Medical Press Limited. The full terms of this license are available at https://www.dovepress.com/terms.php and incorporate the Creative Commons Attribution – Non Commercial (unported, v3.0) License (http://creativecommons.org/licenses/by-nc/3.0/). By accessing the work you hereby accept the Terms. Non-commercial uses of the work are permitted without any further permission from Dove Medical Press Limited, provided the work is properly attributed. For permission for commercial use of this work, please see paragraphs 4.2 and 5 of our Terms (https://www.dovepress.com/terms.php).

International Journal of Nanomedicine downloaded from https://www.dovepress.com/ by 43.243.61.32 on 17-Oct-2018
For personal use only.

nanofibers.[3,4] However, nanotechnology approach by employing biodegradable electrospun nanofiber has attracted more researchers due to its large surface to volume ratio and high drug encapsulation efficiency.[5–7] More so, the interconnected porosity of electrospun nanofiber plays a significant role in cell attachment and proliferation, thereby inhibiting cancer metastasis when applied locally.[8] The enhanced anticancer efficacy using electrospun nanofiber encapsulated with different therapeutics such as paclitaxel, doxorubicin, and dichloroacetate has been studied in previous reports.[9,10] However, there is still incomplete elimination of tumor due to challenges resulting from inefficient drug permeability in the tumor site and drug resistance of tumor cells by employing electrospun nanofiber loaded drug alone.[11,12] Photothermal therapy (PTT) is one of the promising supplements in traditional cancer therapy that utilized laser-induced hyperthermia ablation of cancerous cells.[13–15] It employs a photo-absorbing agent that converts light energy into heat, in a given system, to kill cancer cells.[16] Near-infrared (NIR) radiation has been successfully used in photothermal therapy due to its deeper penetration depth in biological tissues.[17] Nonvascular interventions such as gastroscopy and endoscopy have been employed simultaneously with NIR to eradicate oral, skin, colon, and esophageal cancers.[18] Though conventional NIR agents such as carbon nanotubes (CNTs), gold (Au) nano-rods, and quantum dots have been used as drug carriers for a combination of chemo and thermotherapy, they present some health risks due to non-biodegradability/nontarget accumulation and thus are toxic to some extent in the biological environment.[19–21] Also, coupled with longer therapy duration due to slow heating of most of these photothermal agents could cause sever discomfort to the patients during administration as they usually take between 5 and 20 minutes.[22,23] Hyperthermia has been employed synergistically to annihilate cancer cell as well as increase drug penetration in the tumor sites.[24] Therefore, on this ground, it is highly desirable to develop an efficient multimodal tumor synergistic chemo and phototherapy with reduced side effects and duration of therapy.

Melanin is a naturally occurring pigment virtually present in all living organisms. This material can be employed as a probe due to its abundant multifunction coupled with molecular imaging. Also, its excellent biocompatibility, strong photothermal conversion, water dispersibility, and non-cytotoxic properties have raised interest among many researchers.[25–27] In vivo study of polydopamine nanospheres (PD NPs), which have similar characteristics to melanin, had demonstrated that it could be an excellent drug delivery system and can be used in image-guided chemotherapy.[28]

Bortezomib (BTZ) was chosen as a chemotherapy drug because of its enhanced cytotoxicity with hyperthermia.[29] The toxicity effect arose as a result of its cytostatic effect coupled with induced apoptosis.[30]

Polydioxanone (PDO) is emerging as an attractive absorbable polymer in the biomedical field due to its excellent biodegradability. Also, when coupled with the ester bond and the ether functionality in the polymer chain, it also offers a good flexibility to the material. Typically, this polymer follows hydrolytic degradation due to the presence of ester bond and yields low molecular weight acid species, which can be bioabsorbed by the body.[31] PDO is completely absorbed within 240 days without tissue inflammation compared to other bioabsorbable polymers like polylactic acid and polyglycolic acid that shows some degree of tissue inflammation due to the release of severe acidic component during degradation.[32,33] Furthermore, PDO loses half of its strength after 4 weeks of in vivo implantation.

The purpose of this study was to design an electrospun nanofiber-based local drug delivery system for combined chemo and photothermal therapies. The combination of BTZ and PD NPs in electrospun PDO nanofiber through environmental friendly electrospinning method was developed for the first time and analyzed by in vitro studies. The device is expected to be implanted in order to maintain contact with the tumor site directly, thus enabling continuous localized heating and drug release.

Materials and methods

Most chemicals were purchased from Sigma Aldrich Co. (St Louis, MO, USA), unless otherwise stated. PDO (Resomer® X 206 S), BTZ (Santa Cruz Biotechnology Inc., Dallas, TX, USA), and PD NPs (PD diameter: 250–280 nm) were synthesized according to our previous report.[34] 1,1,1,3,3,3-hexafluoroisopropanol (HFIP) was purchased from Tokyo Chemical Industry Co., Ltd. (Tokyo, Japan). All reagents were used as received, and the solution was prepared in ultrapure water purified with a Milli-Q UV Plus water purification system (EMD Millipore, Billerica, MA, USA).

Fabrication of electrospun drug-loaded nanofibrous scaffolds

First, HFIP (8 mL) was added into a vial containing 30 mg PD NPs followed by tip sonication for 20 minutes resulting in a brown solution. After dispersion of PD NPs, 80 mg of BTZ was added and allowed to dissolve for another 1 hour at room temperature. PDO (15% w/v, 1.2 g) was added into the resultant suspension and stirred overnight for complete dissolution before electrospinning.

The parameters for electrospinning were as follows: electric field: 14.2 kV; air gap distance: 80 mm; flow rate: 6 mL/h; mandrel rotation speed: 1,265 rpm; and all experiments were

International Journal of Nanomedicine downloaded from https://www.dovepress.com/ by 43.243.61.32 on 17-Oct-2018
For personal use only.

conducted at room temperature. The contents of BTZ and PD NPs were 7% and 2.5% with respect to PDO weight after optimization. Residual solvent was removed from all composite fiber by placing them in a vacuum oven at room temperature for 48 hours.

Fourier-transform infrared spectroscopy (FTIR) measurement

The surface chemistry was analyzed by FTIR in the range 4,000 to 250 cm^{-1} on a PerkinElmer spectrophotometer (PerkinElmer Inc., Waltham, MA, USA), in a single attenuated total reflection (ATR) mode at room temperature.

Heat generated by PDO nanofiber and PD NPs

The heat generated from PDO nanofiber under 808 nm NIR (2 W/cm^2) was studied. The composite fibers were immersed in 1× PBS (pH 7.4, 300 µL) and irradiated at various time intervals, while the temperature of the medium was measured by a thermal camera equipped with a LabVIEW real-time acquisition program. The same procedure was employed for PD NP solution (300 µL). For each consecutive test, the temperature was equilibrated to room temperature. The thermal reversibility of the PDO nanofiber was investigated by NIR irradiation (2 W/cm^2) for 60 seconds "on" and allowing the solution temperature to equilibrate to room temperature "off" which took an average of 300 seconds for each cycle.

T_g of the composite fibers

The glass transition temperature (T_g) of the composite fibers were analyzed by differential scanning calorimeter (DSC; PerkinElmer Inc.). The heating rate was adjusted to 10°C/min, and the samples were subjected to cycles of heating up to 140°C and cooling to −40°C.

Hydrolytic degradation test

The hydrolytic degradation of the PDO nanocomposites was performed in 5 mL of PBS (pH 7.4). The samples were placed in a 50-mL test-tube containing the buffered solution and were immersed in a water bath at 37°C. At predetermined periods (5, 10, 20, 30, 40, 50, 60, and up to 80 days), the samples were removed from the buffered solution, rinsed with deionized water, dried, and weighed to determine the residual mass. For NIR group, NIR light was irradiated on the samples at a duration of 3 minutes prior to the test (n=3).

Field emission scanning electron microscopy (FESEM)

The morphology of the composite or surface structure of fabricated fibers was studied by scanning electron microscopy (SEM), Bio-transmission electron microscopy (TEM), and FESEM (Zeiss Supra 40VP; Carl Zeiss Meditec AG, Jena, Germany), after evaporation at room temperature.

Tensile test

The tensile properties of the PDO nanofiber and composites were performed on an Instron 3365 testing machine with respect to ISO 1798:2008 standard. Dog-bone-shaped samples were prepared, and the tensile loading rate was set to 20 mm/min.

Static water contact angle

The water contact angle was analyzed by ramé-hart instrument contact angle analyzer (model number: 200-F1). Double-distilled water (H_2O) was used as the probe liquid, and the measurements were carried out at room temperature (20°C). For each membrane, the measurements were repeated thrice (n=3), and the average value was reported.

In vitro BTZ release test

The cumulative BTZ released from PDO nanofiber with and without NIR irradiation was separately analyzed. PDO nanofiber was placed in 5 mL (pH 7.4 – the physiological and pH 5 – the endosomal pH of cancer cells) 1× PBS solution (ethanol/water) at 37°C with mild shaking. At each designated time, 0.5 mL of release medium was pipetted out and replaced with an equal sample of fresh PBS. To probe the effect of NIR on the control release profile of BTZ, nanofiber in the PBS was exposed to 2 W/cm^2 of 808 nm NIR irradiation for 60 seconds. The NIR was turned "off" for 10 minutes followed by pipetting out and replacing 0.5 mL equal sample of PBS. This procedure was repeated for three cycles. The BTZ concentration was measured by UV–vis spectroscopy (SCINCO Mega-800; SCINCO Co., Ltd., Seoul, South Korea, assembled in China) at a wavelength of 270 nm.

In vitro cancer cytotoxicity test

The cytotoxicity of BTZ-loaded composite fiber was performed to evaluate the efficiency to induce cell death toward CT26 cancer cells (supplied by Korean Cell Line Bank, Seoul, South Korea). Prior to cell seeding, the PDO nanofibers assembled on a 10-mm cover slip were sterilized for 10 minutes in a PBS (pH 7.4) and was later transferred into a 48-well plate. The cells were cultured using DMEM (Thermo Fisher Scientific, Waltham, MA, USA) supplemented with 10% FBS (Thermo Fisher Scientific) and 1% penicillin–streptomycin at 37°C in 5% CO_2 atmosphere. The duration of culture was 1, 3, and 5 days and the drug contained in the nanofiber-loaded mat was 340 µg of BTZ. A density of 5×10^3 cells per well was incubated on the fiber mats at

International Journal of Nanomedicine downloaded from https://www.dovepress.com/ by 43.243.61.32 on 17-Oct-2018
For personal use only.

37°C. The combined effect of PTT and chemotherapy was evaluated following 2 W/cm^2 of 808 nm NIR irradiation. After 48 hours, each sample was irradiated with 2 W/cm^2 of 808 nm NIR for 3 minutes, and the corresponding cell viability was evaluated by cell counting kit-8 (CCK-8) assay at 24, 48, and 72 hours. Finally, LIVE/DEAD® assay was employed to stain the samples which were later examined under confocal microscopy (Carl Zeiss Meditec AG).

Statistical analysis

In this study, we repeated each experiment at least three times. All the quantitative results were reported as mean ± SD. Statistical analysis was carried out by means of one-way ANOVA. Statistical significance was accepted at P-value <0.05.

Results

Figure 1 presents the schematic representation from fabrication to combined chemo and photothermal cancer annihilation of BTZ-loaded nanofiber containing lethal PD NPs.

The morphology of the PDO nanocomposite fibers was characterized using SEM. Figure 2A and A^1 shows that electrospun neat PDO mat formed a fibrous structure with evenly distributed fibers in a random woven structure similar to PDO composite and each set having an average diameter of 2.3±0.2 µm. PDO nanofiber structure was maintained even after the incorporation of PD (2.5 W%) though resulted in a mildly rough surface due to the protrusion of some PD NPs well encapsulated inside the fibers as depicted in Figure 2B and B^1 (red arrow). We further confirmed this with Bio-TEM and SEM images (Figure S1; red arrow and yellow circles) as fewer PD NPs could be observed closer to the surface of the fiber, which was because the solution processed electrospinning method. However, increasing the concentration of PD (5% and 10%) in the matrix resulted in the formation of crumps or agglomerates supported by polymer fiber coupled with intermittent nozzle blockage (Figure S2). Morphological changes after NIR irradiation to PDO composite fiber after 60 and 300 seconds in Figure 2C, C^1, D, and D^1, respectively, showed that the fiber intersection points melted and fused together forming a web-like structure. This fusion is more prominent after 300 seconds as most of the intersections are fused compared to 60 seconds irradiation samples. This clearly showed that the plasmonic heat generated by PD was much higher than the micro-melting point of PDO seen around 46.9°C as indicated by DSC plot. However, in the case of PDO nanofiber without PD, no melting or fused intersections were observed after irradiation, as shown in Figure S3, due to the absence of a photothermal agent.

DSC was used to analyze the heating property of PDO, PDO+PD, and PDO+PD-BTZ as represented by the first

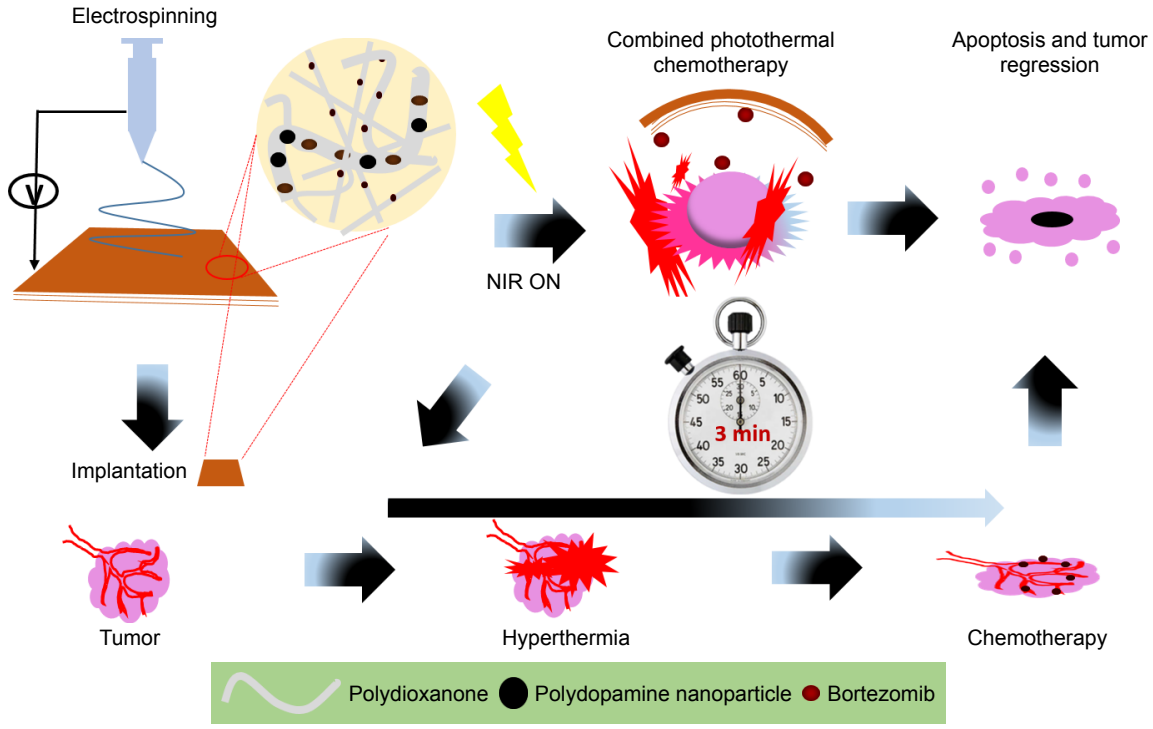

Figure 1 A schematic illustration from material fabrication to tumor ablation using a single hybrid nanofiber platform for synergistic anticancer treatment via simultaneous PTT and chemotherapy.
Abbreviations: NIR, near-infrared; PTT, photothermal therapy.

International Journal of Nanomedicine downloaded from https://www.dovepress.com/ by 43.243.61.32 on 17-Oct-2018
For personal use only.

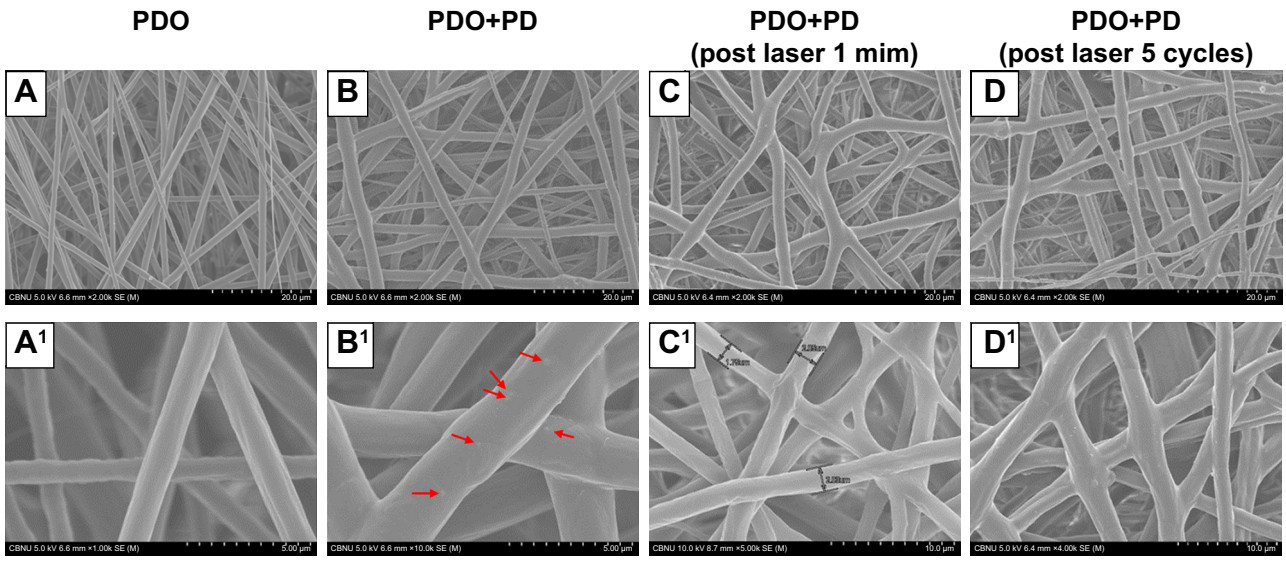

Figure 2 Morphological changes in PDO nanofiber device.
Notes: (**A**) PDO nanofiber. (**B**) PDO+PD. (**C**) PDO+PD after laser irradiation for 60 seconds. (**D**) PDO+PD after five cycles of laser irradiation at 60 seconds per cycle. (**A**^{1}) The smooth surface of PDO. (**B**^{1}) PDO+PD surface with visible particles finely distributed and marked with red arrow. (**C**^{1}) PDO+PD shows a gross surface of nanofiber with minimal fused intersections after 60 seconds of laser irradiation. (**D**^{1}) PDO+PD fiber surface with most of the intersection fused.
Abbreviations: PD, polydopamine; PDO, polydioxanone.

heating DSC scans in Figure 3. The melting point of PDO was not altered by the electrospinning process (106.06°C; Figure 3A). A closer look at the graphs in Figure 3B shows four characteristic transitions: 1) the glass transition peak, 2) a micro-melting peak, 3) crystallization peak, and 4) the melting peak of −3.19°C, 46°C, 81.80°C, and 106.06°C, respectively, for neat PDO sample. This result is similar to the previous report on PDO nanofiber.[35] Also, PDO has been reported to undergo partial melting and recrystallization when heated, which could appear as an exotherm right before the broad melting peak in DSC scan.[36] However, incorporation of PD in the PDO nanofiber resulted in transition shift to higher temperatures as observed in the thermograph. This shift was also noticeable for a sample containing BTZ as the T_g and

A

Sample	T_g (onset)(°C)	T_g (mid point)(°C)	T_c (°C)	T_m (°C)	H_m (J/g)	H_c (J/g)	% crystallinity
PDO	−11.03	−3.19	81.80	106.06	59.59	3.74	59.54
PDO+PD	−11.96	−1.73	81.52	106.00	58.68	3.36	58.63
PDO+PD+BTZ	−8.94	−4.95	81.26	107.03	60.07	4.45	60.00

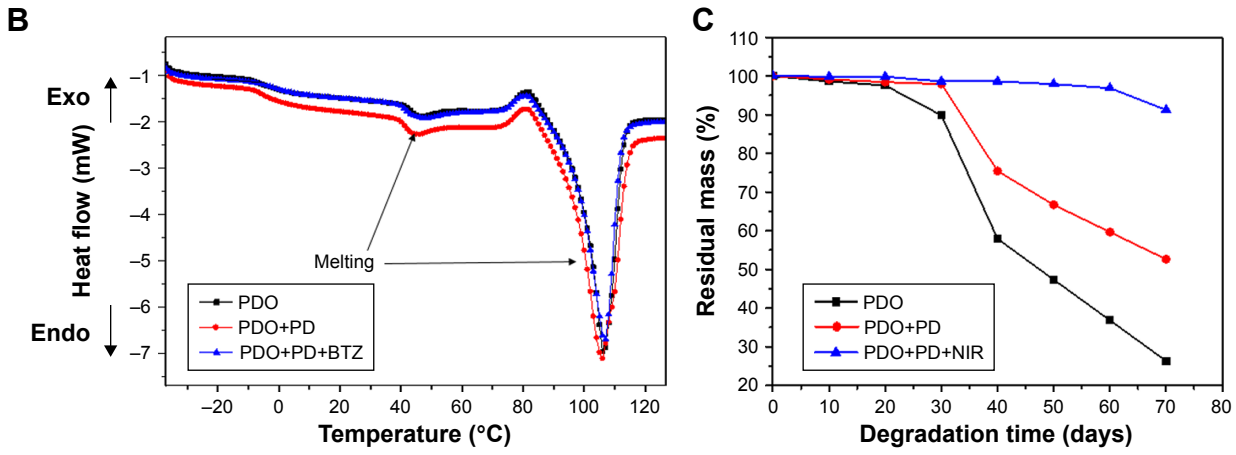

Figure 3 DSC and degradation property of various composite fibers.
Notes: (**A**) Variation in glass transition and other heating properties of various fibers. (**B**) Heat flow of various fiber mats. (**C**) Weight loss of PDO nanocomposites over 80 days in PBS (pH 7.4).
Abbreviations: BTZ, bortezomib; DSC, differential scanning calorimeter; PD, polydopamine; PDO, polydioxanone; NIR, near-infrared; T_g, glass transition temperature; T_c, crystallization temperature; T_m, melting temperature; H_m, enthalpy of melting; H_c, enthalpy of crystallization.

International Journal of Nanomedicine downloaded from https://www.dovepress.com/ by 43.243.61.32 on 17-Oct-2018
For personal use only.

melting peaks were raised to −8.94°C and 107.03°C, respectively (Figure 3A).

We further evaluated the degradation behavior of PDO nanocomposite fibers to understand the effect of NIR irradiation on hydrolytic degradation profile (Figure 3C). It was clearly observed that neat PDO nanocomposite lost ≈50% of its weight after 50 days of incubation. This is typical for electrospun PDO sample as water would penetrate into the hydrophilic matrix thereby inducing chain scission or hydrolysis of the ester bonds.[37] However, incorporating PD into the nanofiber suppressed the degradation rate as 67% residual weight was obtained on the 50th day. This might be due to the strong interactions (possibly hydrophobic and hydrogen bonding) between PD and PDO matrix which delayed the hydrolytic degradation process. Interestingly, the NIR irradiated sample showed much suppressed degradation rate as 96% residual weight was observed after 60 days. The reason might be that the webbed network fiber structure formed after irradiation as discussed in FESEM can minimize the amount of trapped water and, therefore, slow down the permeation of water into the polymer, thus inhibiting the rate of degradation. These results were also confirmed by SEM (Figure S4) after 10, 20, and 30 days. Surface roughening of PDO fiber could be observed after 10 days, which resulted in mild fiber breakage at 20th day. However, on 30th day the neat PDO fiber breakage was more obvious in contrast to PDO+PD and PDO+PD+NIR, confirming our hypothesis that PD interaction and NIR irradiation suppressed the degradation rate.

Photothermal conversion or stability of PD NPs and PDO composite fiber

Figure 4A presents the SEM morphology of the PD NPs synthesized in this study. The particle was brown colored and spherical in shape with partially mono-dispersed size distribution of around 260±10 nm, typical to melanin reported in previous studies.[38] Different concentrations of PD NPs were prepared in PBS as presented in Figure 4B which showed that as the concentration of the particles increases, the intensity of the resultant solution is also increased. As clearly observed in Figure 4C and D, before and after five cycles of NIR irradiation on PD NPs, there were no observable changes in morphology, implying robustness of the particles against photobleaching unlike other photothermal agents like gold nanoparticles.[39] Further we look at the photothermal properties of PD NPs in PBS during irradiation. Since the photothermal effects occur due to heating of materials after light absorption, the ability of a material to absorb optical energy can result in the release of other forms of energy, like electrical energy and heat energy. Therefore, photothermal heating of a sample often results in a temperature rise coupled with the release of other wave forms simultaneously. Figure 4E shows that various PD NP solutions released a large amount of heat than PBS (used as a control). Interestingly, temperature change (ΔT) between highly concentrated PD solution (1,000 μg/mL) and PBS reached ≈16°C after 10 seconds of NIR irradiation. As observed, the concentration of PD correlates well with heat generated. However, PDO composite nanofiber showed much higher heat generated (ΔT =30°C) after 10 seconds of irradiation in contrast to PBS. It should be noted that the weight of PDO nanofiber (5 mg ≡ 420 μg/mL PD in PBS) was lower than that of NIR-heated PD solution (1,000 μg/mL) though generated higher photothermal conversion. This is likely due to closely packed PD NPs in PDO composite fiber resulting in a large surface area for light absorption compared to sparsely distributed PD NPs in the solution. The high heating stability of PDO nanofiber might probably be due to high fiber flexibility and robustness of PD NPs and soft PDO polymer shell. These results clearly showed that NIR-induced PDO nanofiber was able to effectively convert light into high thermal energy with excellent heating capability. The process of NIR-triggered exothermy of PDO nanofiber could possibly involve optically stimulated resonance or quantum confinement effect caused by PD NPs resulting in rapid heating similar to photo-induced metal nanoparticles.[40] The photothermal stability of PDO nanofiber was assessed by time-dependent temperature variation upon NIR irradiation for 60 seconds followed by natural cooling to room temperature at each cycle after NIR was turned "off." Figure 4F clearly shows that after five cycles of NIR irradiation, there is no noticeable decline in photothermal conversion which confirmed the good photo stability of the PDO composite. Upon irradiation, the temperature could rise up to 50°C within 60 seconds and take an average of 300 seconds to cool down to room temperature when NIR laser was turned "off." The excellent photothermal performance observed in these results demonstrates the ability of the device to arrest tumors undergoing metastasis.

Due to the versatility of NIR technology, numerous reports in the biomedical field have found it attractive owing to its transparency to biological systems.[41] Here we explore the optical properties of PDO nanofiber and PD NPs under NIR light irradiation using the thermal camera. Figure 5A shows the thermographic image of 300 μL of 50 μg/mL PD NP solution with a maximum temperature of 28.7°C. However, increasing the concentration to 100, 500, and 1,000 μg/mL yields a maximum temperature of 31.6°C, 47.7°C, and 53.3°C, respectively (Figure 5B–D) after 60 seconds of irradiation. In contrast, neat PDO fiber alone was not responsive to NIR (Figure 5E, inset), whereas PDO composite fiber shows a rapid increase in temperature up to 63°C within 60 seconds of irradiation (Figure 5F; Movie S1).

International Journal of Nanomedicine downloaded from https://www.dovepress.com/ by 43.243.61.32 on 17-Oct-2018
For personal use only.

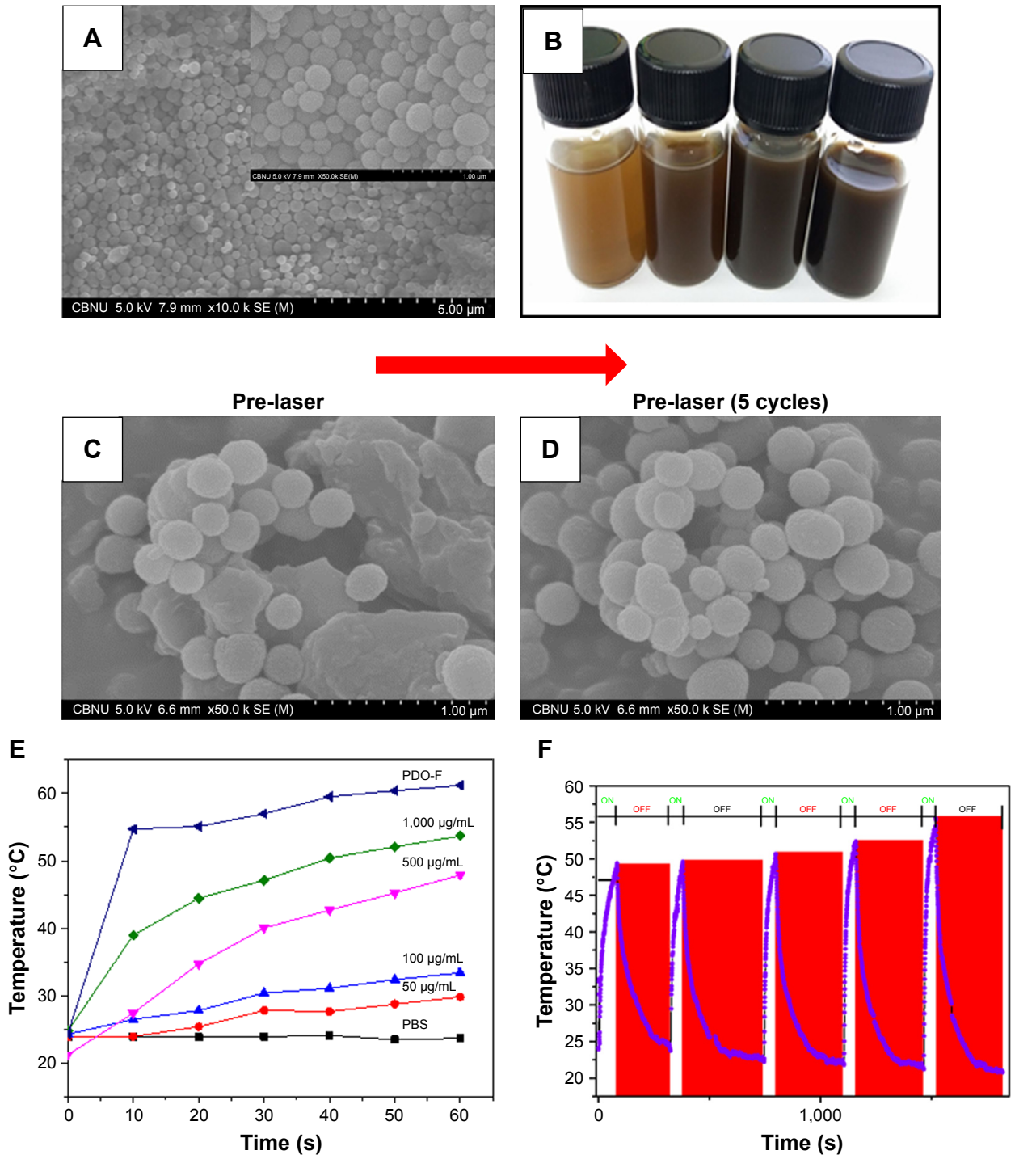

Figure 4 Characterization of PD NPs and photothermal stability testing.

Notes: (**A**) SEM image of PD NPs (inset – the magnified image of **A**). (**B**) A vial containing an aqueous suspension of various concentrations of PD (50, 100, 500, and 1,000 µg/mL). (**C** and **D**) Stability of PD NPs before and after five cycles of laser irradiation (2 W/cm^2; 808 nm at 60 seconds per cycle). (**E**) Effect of concentration on the photothermal output of PD NPs at 60 seconds irradiation (808 nm; 2 W/cm^2). (**F**) High precision thermal cycle by nonstop laser on–off switching on PDO composite fiber. The blue and red zones as indicated represent "on" and "off" modes, respectively. The sample was irradiated with 808 nm laser at the power of 2 W/cm^2 for 60 seconds ("on") followed by natural cooling for 300 seconds ("off").

Abbreviations: PD NPs, polydopamine nanospheres; PDO, polydioxanone; SEM, scanning electron microscopy.

Cytotoxicity or average fiber diameter

SEM image of the PDO composite nanofiber surface (Figure 2A) shows a uniform randomly oriented fiber with an average diameter of 2.3±0.2 µm (Figure 6A) analyzed by ImageJ software. We further tested the possible toxicity of PD NPs upon incubation with CT26 cancer cells. CT26 cells were first preincubated with PD NPs at various concentrations (100, 500, and 1,000 µg/mL) for 48 hours. PD NPs show

International Journal of Nanomedicine downloaded from https://www.dovepress.com/ by 43.243.61.32 on 17-Oct-2018
For personal use only.

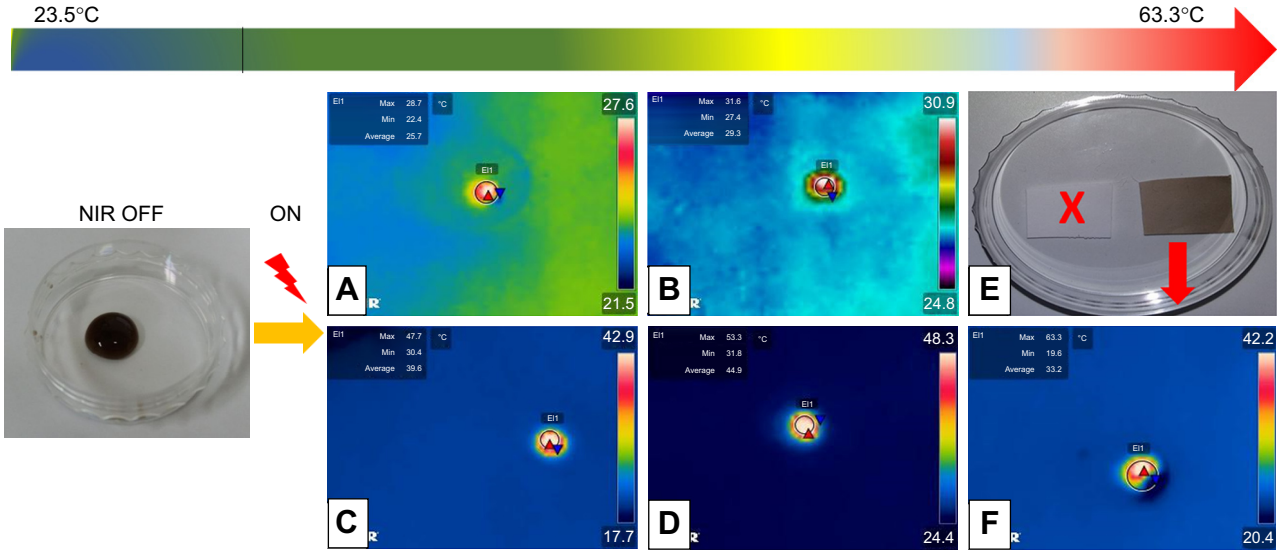

Figure 5 Laser-induced heating on different concentrations of PD NP solution and composite fiber.
Notes: (**A**–**D**) Thermographic images of PD NP solution droplet (300 µL of 50, 100, 500, and 1,000 µg/mL, respectively) after NIR irradiation. (**E**) Digital image of fabricated nanofiber device (white – neat PDO fiber mat and brown – with PD NPs [3.8 mg/mL]) (**F**) Thermographic image was captured from respective Movie S1 showing PDO composite nanofiber device (0.005 mg) in 300 µL PBS. Power and wavelength of the NIR light used in this study were the same for all samples, that is, 2 W/cm² and 808 nm, respectively, for 60 seconds irradiation time. All images are screenshots captured from respective movies.
Abbreviations: NIR, near-infrared; PD NPs, polydopamine nanospheres; PDO, polydioxanone.

no sign of toxicity even at high concentration (Figure 6B; 1,000 µg/mL) (cells were viable >90%) in contrast to other photothermal agents reported elsewhere which show high toxicity in high dose.[19] The low toxicity of PD NPs was also reported by numerous researchers in both in vivo[42] and in vitro studies.[43]

Surface or mechanical property of nanofiber

ATR-FTIR was carried out to evaluate the surface characteristics of the PD, PDO, and PDO+PD-BTZ (Figure 7A). PD show a typical characteristic peak at around 3,500 and 1,682 cm^{-1}, which belongs to catechol (C–OH) and amine

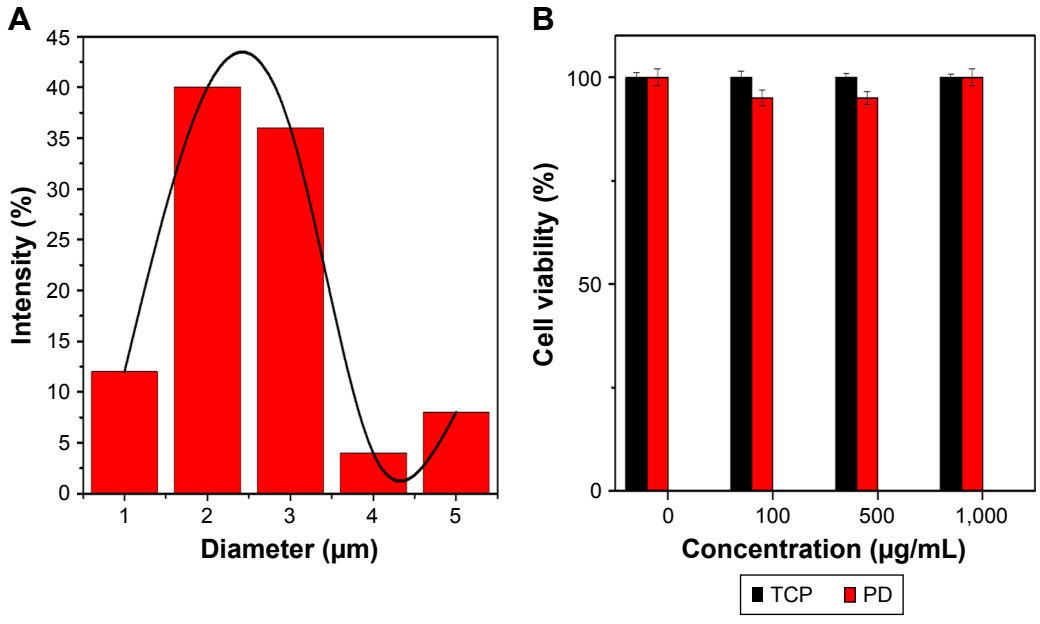

Figure 6 (**A**) Fiber diameter distribution in the fabricated photothermal device. (**B**) Cell viability following treatment with various concentrations of PD NPs and using TCP as control after 48 hours culture.
Note: Error bar represents SD of three independent measurements.
Abbreviations: PD, polydopamine; PD NPs, polydopamine nanospheres; TCP, tissue culture plate.

International Journal of Nanomedicine downloaded from https://www.dovepress.com/ by 43.243.61.32 on 17-Oct-2018
For personal use only.

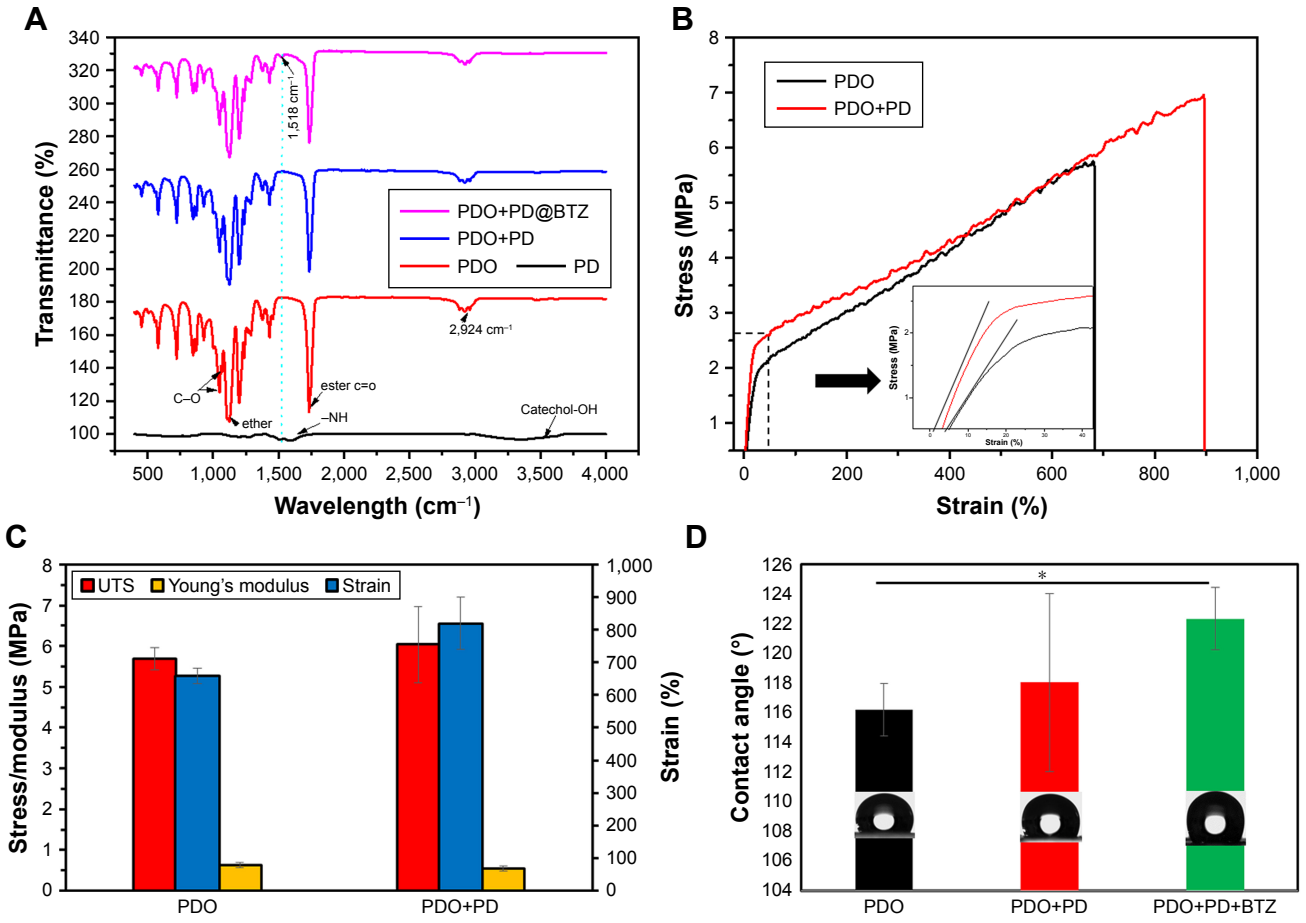

Figure 7 Mechanical property and chemical component of composite fiber (**A**) ATR-IR. (**B**) Stress–strain curve. (**C**) Mechanical property. (**D**) Contact angle.
Note: *$P<0.05$.
Abbreviations: ATR, attenuated total reflection; BTZ, bortezomib; IR, infrared; PDO, polydioxanone; PD, polydopamine; UTS, ultimate tensile strength.

(–NH) functionalities, respectively. PDO shows a typical characteristic peak at 1,730 cm^{-1} which represent the ester carbonyl group (C=O), 1,117.8 cm^{-1} belongs to the shoulder broadening of the ether group, 1,052 and 1,066 cm^{-1} belong to a C–O band of ester, whereas the peak at 2,925 cm^{-1} is the characteristic of the aliphatic group. The amorphous and crystalline phases of polyesters are denoted at the finger print region, 452, 507, 580, 723, 840, 873, and 929 cm^{-1}. The spectra of PDO nanofiber incorporated with PD show a characteristic N–H sharing band at 1,518 cm^{-1} of polydopamine which becomes prominent on BTZ containing sample due to the presence of N–H functionality.

The mechanical strength of the PDO composite fibers was investigated by the tensile stress–strain testing method. The stress–strain curves of PDO and PDO fiber incorporated with PD are presented in Figure 7B, and their young modulus, tensile strength, and elongation at break are represented in the multiple bar chart (Figure 7C). The plot clearly shows that after the incorporation of PD, increased ultimate tensile strength and elongation at break from 5.6 MPa (658%) to 6 MPa (819%), respectively, with 12% reduction in young modulus were observed. The improvement in mechanical properties was a result of PD incorporation which acted like a rigid nanofiller normally used in the mechanical enhancement of polymer.[44] Other nanofillers widely employed to enhance polymeric composite are graphene, functionalized magnetic nanoparticle, and carbon nanotube.[45–47] The principle of improving composite materials by nanofillers is based on stress transfer from filler to the composite matrix, which is mostly dependent on uniform dispersion and strong interaction between the nanoparticle and the matrix.[48,49] PD has predominant N–H and partial C=O (quinone due to oxidation) on the surface as demonstrated in the ATR-FTIR result. As previously reported, hydrogen bonding is often common in the composite as one necessary type of matrix–filler interaction. Therefore, hydrogen bond formation between PD (N–H) and PDO composite matrix (C=O) is probably responsible for improved mechanical properties though other physical bonding like hydrophobic interaction and π–π stacking cannot be ignored.

International Journal of Nanomedicine downloaded from https://www.dovepress.com/ by 43.243.61.32 on 17-Oct-2018
For personal use only.

Therefore, these data show that the presence of biomimetic PD in PDO nanofiber shows enhanced mechanical property than neat PDO nanofiber.

Contact angle

Surface wettability plays a significant role in the interaction of cells with any biomaterial. As shown in Figure 7D, the water contact angle for neat PDO is found to be ≈116°±2°; however, incorporation of PD shows a mild increase up to 118°±6°, which indicates that the surface of the fiber mats is hydrophobic. This effect is similar to the observation found in the incorporation of CNT in polycaprolactone nanofiber.[50] Finally, the PDO composite fiber containing BTZ shows enhanced hydrophobicity up to 122° due to the hydrophobic nature of BTZ, which made it possible for specific inhibition of the chymotrypsin-like site that significantly reduces protein processing and inhibits tumor cell proliferation, induce apoptosis, and inhibit angiogenesis.[51]

In vitro drug release studies

Here we investigated the in vitro drug release behavior of PDO composite fiber without NIR irradiation in PBS at 37°C by two pH values (5 and 7.4) in order to mimic the endosomal pH and physiologic condition, respectively (Figure 8A). It is clear that BTZ release was restricted in pH 7.4 over 30 hours, as only 9.6% BTZ was released into the media, whereas at pH 5, burst release was observed as 100% of the drug got released within 6 hours. These data show that BTZ solubility increases with a decrease in pH, which is similar to the extracellular space with the tumor tissue and lysosomes as previously reported.[52,53] Also, the strong conjugation of BTZ with the remaining unoxidized catechol-OH group on the PD could also account for slower drug release in pH 7.4, while at lower pH 5, the groups could dissociate resulting in a faster release. We also studied the drug release profile using NIR (2 W/cm^2) irradiation as remote controlled "on" and "off" switches in pH (7.4 and 5) at 37°C. Figure 8B shows the remote-controlled release profile in response to "on" and "off" switches of NIR light. It clearly showed that the slow release profile of BTZ was observed in pH 7.4, where ~1% of the drug was released within the first cycle (60 seconds of NIR irradiation). However, a burst release of loaded BTZ was observed in pH 5 with a total amount of 70% after 60 seconds of irradiation time. In contrast, 100% BTZ was released in pH 5 after second cycle, whereas 2% in pH 7.4 after the second cycle was released. More so, in both pH values, BTZ release profile returned back to its slow release pattern after the NIR was switched "off." The effective NIR-induced on-demand release of BTZ has been employed by other researchers using multiwalled carbon nanotube,[54] silica–gold nanoparticle,[55] and GO.[56] However, it is also worthy to mention that the safety and toxicity concerns of other photothermal agent were significantly higher as confirmed by the previous reports[19] in contrast to PD used in this study. Since diffusion is the typical drug release mechanism for drug-loaded fibers at an early stage and due to moderate degradation of PDO, the

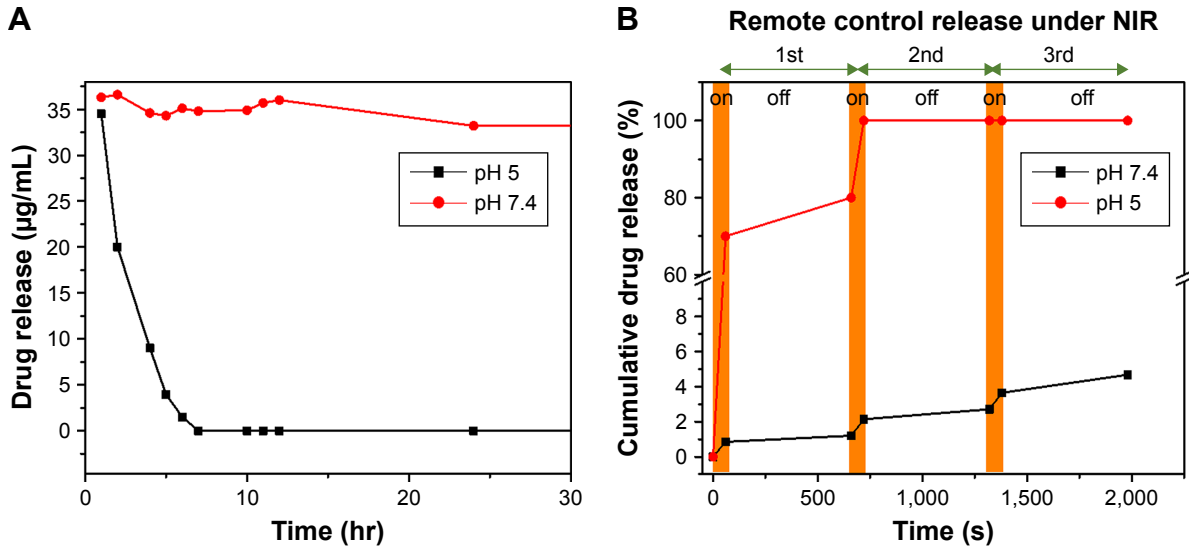

Figure 8 In vitro BTZ release profile from PDO composite fiber under acidic, basic, and NIR control conditions in PBS at 37°C.
Notes: (**A**) Release profile under acidic (pH 5) and basic conditions (pH 7.4). (**B**) Under NIR irradiation (pH 7.4). The brown zone represents NIR "on" each at 60-second duration.
Abbreviations: BTZ, bortezomib; NIR, near-infrared; PDO, polydioxanone.

International Journal of Nanomedicine downloaded from https://www.dovepress.com/ by 43.243.61.32 on 17-Oct-2018
For personal use only.

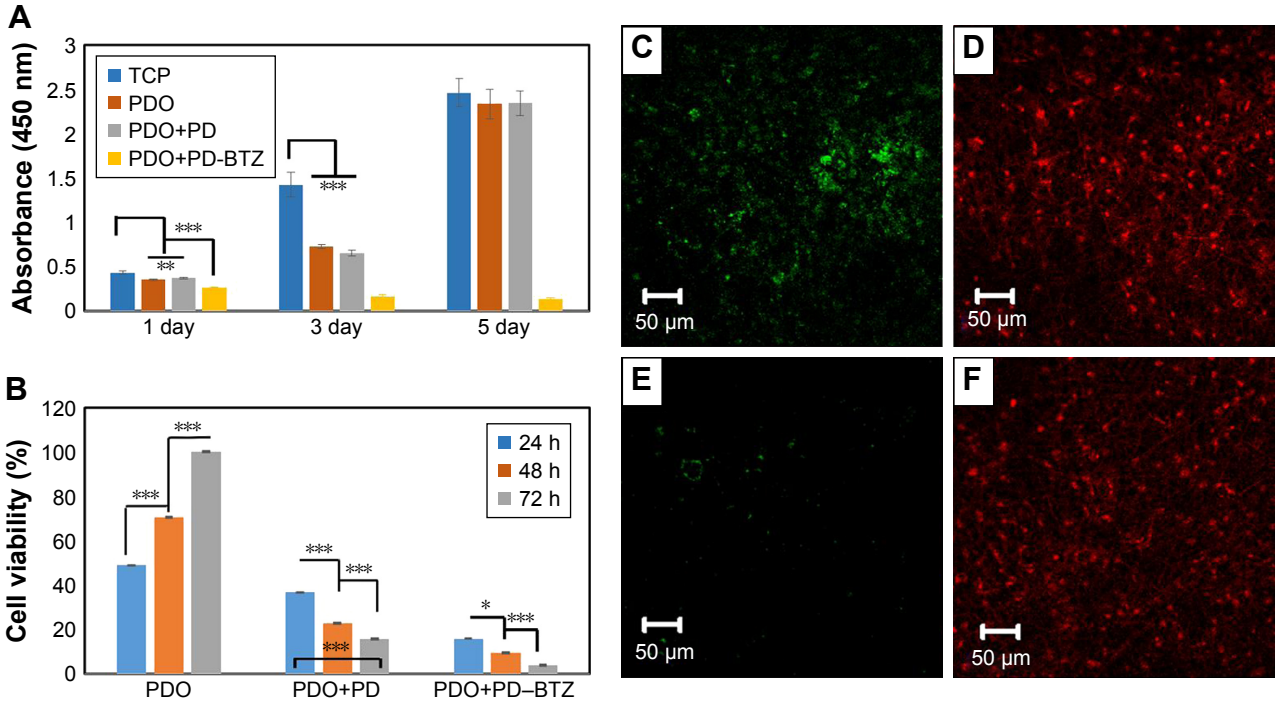

Figure 9 Cell viability indices of combined therapy and the effect of treatment on cancer cells assessed by LIVE/DEAD® assay with CT26 cancer cells.
Notes: (**A**) Histogram showing CCK-8 data (OD) of CT26 cancer cell viability for control and therapy groups with no irradiation on 1, 3, and 5 days. (**B**) The viability of CT26 colon cancer cell co-incubated with PDO, PDO+PD, and PDO+PD-BTZ. (**C** and **D**) LIVE/DEAD® cell microscopic images of PDO+PD nanofiber after 72 hours of treatment. (**E** and **F**) Combined photothermal and chemotherapy treatment using PDO+PD-BTZ nanofiber after 72 hours of treatment. One-way ANOVA post hoc Tukey test was used to indicate the significance (*$P<0.05$, **$P<0.01$, and ***$P<0.001$).
Abbreviations: BTZ, bortezomib; PDO, polydioxanone; PD, polydopamine; TCP, tissue culture plate; OD, optical density; CCK-8, cell counting kit-8.

polymer chain mobility plays a critical role.[57] Since bulk PDO nanofiber is a semicrystalline material,[31] DSC results demonstrate that incorporation of PDO and BTZ does not change the crystallinity greatly, meaning that the BTZ was well dispersed in the matrix.

To demonstrate the mechanism of burst release of BTZ under NIR irradiation, as illustrated in the DSC result, the glass transition temperature of PDO was maintained way below room temperature (around −3.19°C) with micro-melting at 45°C. Therefore, to increase the mobility of the PDO chain, the temperature of the system must exceed this temperature. Hence, upon NIR irradiation, PD could convert light energy into plenty of heat, thereby raising the temperature of the system up to 63°C, which is above the micro-melting temperature. At this temperature, the mobility of the polymer chain could increase, leading to a loosened fiber structure, thus enhancing the drug diffusion rate, with NIR "on" at each 60-second duration.

Cytotoxicity or combined chemo–photothermal therapy test

Cytocompatibility of PDO nanocomposite fiber was analyzed by CCK-8 assay against CT26 cancer cells after 1, 3, and 5 days (Figure 9A). It was observed that all samples except composite incorporated with BTZ were biocompatible as cocultured cells showed exponential growth over time. This result also proved high safety and suitability of PDO nanofiber as a drug carrier. However, the sample containing BTZ showed a decline in growth rate of cells over time due to antineoplastic activity effect of the drug to CT26 cancer cells. The mechanism of BTZ action on cells is usually due to its ability to reversibly inhibit the 26S proteasome responsible for protease complex that degrades ubiquitinated proteins,[51] thus disrupting various cell signal pathways, leading to cell cycle arrest, apoptosis, and suppression of angiogenesis.[51]

Since we have assessed the biocompatibility and therapeutic effect of BTZ on CT26 cells, now it would be interesting to evaluate the combined effects of chemotherapy and hyperthermia. Here cells incubated on PDO composite fibers were irradiated with 2 W/cm^2 of 808 nm NIR for 3 minutes, and the viability was assessed by CCK-8 assay at 24, 48, and 72 hours (Figure 9B). For PDO nanofiber alone (control), an incremental cell growth was observed as it contains neither photothermal agent (PD) nor BTZ. However, the sample containing PD showed a viability of ≈20% after 72 hours

International Journal of Nanomedicine downloaded from https://www.dovepress.com/ by 43.243.61.32 on 17-Oct-2018
For personal use only.

indicating a minimal killing of cancer cells by hyperthermia. In the case of PDO composite fiber containing BTZ, the effect of NIR irradiation reduced the viability of cancer cells down to around 5% after 72 hours showing the efficiency of combination therapy on the elimination of cancer cells. However, due to higher photothermal conversion that may negatively affect normal cells above 46°C, irradiation was employed with 1 second "off" and 2 seconds "on" after initial 9 seconds of continuous irradiation to maintain the temperature between 42°C and 46°C, over 3 minutes of treatment using 2 W/cm^2; 808 nm laser, which resulted in similar cell death (Figure S5A–C). This was due to fast photothermal conversion of PD NPs that can raise the temperature up to 45°C within 9 seconds in contrast to other photothermal agents that show slow heating (43°C within 5 minutes of initial constant irradiation).[58] This enhanced anticancer efficiency using the single platform of PDO composite fiber containing drugs can mostly be observed in chemotherapy effects of BTZ on cancer cells, due to its inhibitory effect on nuclear factor-kappa B that is usually activated by cancer cells for survival. LIVE/DEAD® assay was also employed to confirm our data (Figure 9C–F). The results showed that the group without BTZ (Figure 9C and D) under NIR irradiation after 72 hours still contained a significant amount of green fluorescence (from LIVE cells) in contrast to BTZ containing nanofiber composite which showed a low green fluorescence after 72 hours of NIR treatment (Figure 9E and F). Since these findings confirmed our hypothesis coupled with in vitro cell viability studies, we conclude that employing this single nanofiber composite platform can effectively annihilate cancer cells through chemotherapy and photothermal effects within a short time period, thus offering a more promising opportunity for tumor therapy.

Conclusion

Here we reported a successful combination of chemotherapy and phototherapy integrated into a single platform using electrospun BTZ/PD-loaded PDO fiber mat for synergistic anticancer treatment. It was demonstrated that PD can be encapsulated in PDO nanofiber without any obvious morphological distortion. More so, the PDO containing nanofiber can induce efficient and repeatable heating capacity when exposed to 808 nm NIR light without loss of heating capacity. We further confirm that BTZ containing PDO nanofiber composite allows cancer cell binding, which upon exposure to 3 minutes of NIR irradiation resulted in efficient ablation/elimination of cancer cells. This study provided an interesting prospect of employing drug-loaded nanofiber in a local combination of phototherapy and chemotherapy against CT26 colon carcinoma cells. Since this device can degrade in vivo, the potential long-term side effects to normal tissue and organs can be avoided.

Acknowledgment

This research was supported by grants from the Basic Science Research Program through the National Research Foundation of Korea, funded by the Ministry of Education, Science and Technology (Project nos 2015R1C1A1A02036404 and 2016R1A2A2A07005160).

Disclosure

The authors report no conflicts of interest in this work.

References

1. Wolinsky JB, Colson YL, Grinstaff MW. Local drug delivery strategies for cancer treatment: gels, nanoparticles, polymeric films, rods, and wafers. *J Control Release*. 2012;159(1):14–26.
2. Liu R, Wolinsky JB, Walpole J, et al. Prevention of local tumor recurrence following surgery using low-dose chemotherapeutic polymer films. *Ann Surg Oncol*. 2010;17(4):1203–1213.
3. Sill TJ, von Recum HA. Electrospinning: applications in drug delivery and tissue engineering. *Biomaterials*. 2008;29(13):1989–2006.
4. Jeong B, Bae YH, Lee DS, Kim SW. Biodegradable block copolymers as injectable drug-delivery systems. *Nature*. 1997;388(6645):860–862.
5. Okuda T, Tominaga K, Kidoaki S. Time-programmed dual release formulation by multilayered drug-loaded nanofiber meshes. *J Control Release*. 2010;143(2):258–264.
6. Jin HJ, Fridrikh SV, Rutledge GC, Kaplan DL. Electrospinning Bombyx mori silk with poly(ethylene oxide). *Biomacromolecules*. 2002;3(6):1233–1239.
7. Wang S, Hu F, Li J, et al. Design of electrospun nanofibrous mats for osteogenic differentiation of mesenchymal stem cells. *Nanomedicine*. 2017. Epub 2017 May 26.
8. Huang C, Soenen SJ, Rejman J, et al. Magnetic Electrospun Fibers for Cancer Therapy. *Adv Funct Mater*. 2012;22(12):2479–2486.
9. Liu S, Zhou G, Liu D, et al. Inhibition of orthotopic secondary hepatic carcinoma in mice by doxorubicin-loaded electrospun polylactide nanofibers. *J Mater Chem B*. 2013;1(1):101–109.
10. Xu X, Chen X, Wang Z, Jing X. Ultrafine PEG-PLA fibers loaded with both paclitaxel and doxorubicin hydrochloride and their in vitro cytotoxicity. *Eur J Pharm Biopharm*. 2009;72(1):18–25.
11. Minchinton AI, Tannock IF. Drug penetration in solid tumours. *Nat Rev Cancer*. 2006;6(8):583–592.
12. Petros RA, Desimone JM. Strategies in the design of nanoparticles for therapeutic applications. *Nat Rev Drug Discov*. 2010;9(8):615–627.
13. Jaque D, Martínez Maestro L, del Rosal B, et al. Nanoparticles for photothermal therapies. *Nanoscale*. 2014;6(16):9494–9530.
14. Miao W, Shim G, Kim G, et al. Image-guided synergistic photothermal therapy using photoresponsive imaging agent-loaded graphene-based nanosheets. *J Control Release*. 2015;211:28–36.
15. Wang S, Zhao J, Yang H, et al. Bottom-up synthesis of WS_2 nanosheets with synchronous surface modification for imaging guided tumor regression. *Acta Biomater*. 2017;58:442–454.
16. Zhao P, Zheng M, Luo Z, et al. NIR-driven Smart Theranostic Nanomedicine for On-demand Drug Release and Synergistic Antitumour Therapy. *Sci Rep*. 2015;5:14258.
17. Song G, Wang Q, Wang Y, et al. A Low-Toxic Multifunctional Nanoplatform Based on Cu9S5@mSiO2 Core-Shell Nanocomposites: Combining Photothermal- and Chemotherapies with Infrared Thermal Imaging for Cancer Treatment. *Adv Funct Mater*. 2013;23(35):4281–4292.
18. Lee H, Lee Y, Song C, et al. An endoscope with integrated transparent bioelectronics and theranostic nanoparticles for colon cancer treatment. *Nat Commun*. 2015;6:10059.

International Journal of Nanomedicine downloaded from https://www.dovepress.com/ by 43.243.61.32 on 17-Oct-2018
For personal use only.

19. Chechetka SA, Yu Y, Zhen X, Pramanik M, Pu K, Miyako E. Light-driven liquid metal nanotransformers for biomedical theranostics. *Nat Commun*. 2017;8:15432.
20. Cheng L, Wang C, Feng L, Yang K, Liu Z. Functional nanomaterials for phototherapies of cancer. *Chem Rev*. 2014;114(21):10869–10939.
21. Ma M, Chen H, Chen Y, et al. Au capped magnetic core/mesoporous silica shell nanoparticles for combined photothermo-/chemo-therapy and multimodal imaging. *Biomaterials*. 2012;33(3):989–998.
22. Chu M, Shao Y, Peng J, et al. Near-infrared laser light mediated cancer therapy by photothermal effect of Fe3O4 magnetic nanoparticles. *Biomaterials*. 2013;34(16):4078–4088.
23. Wu CC, Yang YC, Hsu YT, et al. Nanoparticle-induced intraperitoneal hyperthermia and targeted photoablation in treating ovarian cancer. *Oncotarget*. 2015;6(29):26861–26875.
24. Milani V, Lorenz M, Weinkauf M, et al. Combination of hyperthermia and bortezomib results in additive killing in mantle cell lymphoma cells. *Int J Hyperthermia*. 2009;25(4):262–272.
25. Liu Y, Ai K, Liu J, Deng M, He Y, Lu L. Dopamine-melanin colloidal nanospheres: an efficient near-infrared photothermal therapeutic agent for in vivo cancer therapy. *Adv Mater*. 2013;25(9):1353–1359.
26. Liopo A, Su R, Oraevsky AA. Melanin nanoparticles as a novel contrast agent for optoacoustic tomography. *Photoacoustics*. 2015;3(1):35–43.
27. Araújo M, Viveiros R, Correia TR, et al. Natural melanin: a potential pH-responsive drug release device. *Int J Pharm*. 2014;469(1):140–145.
28. Zhang R, Fan Q, Yang M, et al. Engineering Melanin Nanoparticles as an Efficient Drug-Delivery System for Imaging-Guided Chemotherapy. *Adv Mater*. 2015;27(34):5063–5069.
29. Hong YS, Hong SW, Kim SM, et al. Bortezomib induces G2-M arrest in human colon cancer cells through ROS-inducible phosphorylation of ATM-CHK1. *Int J Oncol*. 2012;41(1):76–82.
30. Lioni M, Noma K, Snyder A, et al. Bortezomib induces apoptosis in esophageal squamous cell carcinoma cells through activation of the p38 mitogen-activated protein kinase pathway. *Mol Cancer Ther*. 2008;7(9):2866–2875.
31. Sabino MA, González S, Márquez L, Feijoo JL. Study of the hydrolytic degradation of polydioxanone PPDX. *Polym Degrad Stab*. 2000;69(2):209–216.
32. Laufer N, Merino M, Trietsch HG, Decherney AH. Macroscopic and histologic tissue reaction to polydioxanone, a new, synthetic, monofilament microsuture. *J Reprod Med*. 1984;29(5):307–310.
33. Knoop M, Günstedt B, Thiede A. Maxon and PDS-evaluation and physical and biologic properties of monofilament absorbable suture materials. *Langenbecks Arch Chir*. 1987;371(1):13–28.
34. Obiweluozor FO, Ghavaminejad A, Maharjan B, Kim J, Park CH, Kim CS. A mussel inspired self-expandable tubular hydrogel with shape memory under NIR for potential biomedical applications. *J Mater Chem B*. 2017;5(27):5373–5379.
35. Abhari RE, Mouthuy PA, Zargar N, Brown C, Carr A. Effect of annealing on the mechanical properties and the degradation of electrospun polydioxanone filaments. *J Mech Behav Biomed Mater*. 2017;67:127–134.
36. Dias M, Antunes MC, Santos AR, Felisberti MI. Blends of poly(3-hydroxybutyrate) and poly(p-dioxanone): miscibility, thermal stability and biocompatibility. *J Mater Sci Mater Med*. 2008;19(12):3535–3544.
37. Hakimi O, Murphy R, Stachewicz U, Hislop S, Carr AJ. An electrospun polydioxanone patch for the localisation of biological therapies during tendon repair. *Eur Cell Mater*. 2012;24:344–357.
38. Mbonyiryivuze A, Nuru ZY, Diop Ngom B, Ngom BD, et al. Morphological and Chemical Composition Characterization of Commercial Sepia Melanin. *Am J Nanomaterials*. 2015;3(1):22–27.
39. Pellegrotti JV, Acuna GP, Puchkova A, et al. Controlled reduction of photobleaching in DNA origami-gold nanoparticle hybrids. *Nano Lett*. 2014;14(5):2831–2836.
40. Hirsch LR, Stafford RJ, Bankson JA, et al. Nanoshell-mediated near-infrared thermal therapy of tumors under magnetic resonance guidance. *Proc Natl Acad Sci U S A*. 2003;100(23):13549–13554.
41. Weissleder R. A clearer vision for in vivo imaging. *Nat Biotechnol*. 2001;19(4):316–317.
42. Gu GE, Park CS, Cho HJ, et al. Fluorescent polydopamine nanoparticles as a probe for zebrafish sensory hair cells targeted in vivo imaging. *Sci Rep*. 2018;8(1):4393.
43. Ding YH, Floren M, Tan W. Mussel-inspired polydopamine for bio-surface functionalization. *Biosurf Biotribol*. 2016;2(4):121–136.
44. Roy N, Sengupta R, Bhowmick AK. Modifications of carbon for polymer composites and nanocomposites. *Prog Polym Sci*. 2012;37(6):781–819.
45. Wei Y, Zhang X, Song Y, et al. Magnetic biodegradable Fe3O4/CS/PVA nanofibrous membranes for bone regeneration. *Biomed Mater*. 2011;6(5):55008.
46. Ortiz-Zarama MA, Jiménez-Aparicio A, Perea-Flores MJ, Solorza-Feria J, Barrier S-FJ. Barrier, mechanical and morpho-structural properties of gelatin films with carbon nanotubes addition. *J Food Eng*. 2014;120:223–232.
47. Cai N, Hou D, Shen L, Luo X, Xue Y, Yu F. Functionalization of graphene with hyperbranched polyglycerol for stable aqueous dispersion. *Funct Mater Lett*. 2015;8(6):1550068.
48. Cai N, Li C, Luo X, Xue Y, Shen L, Yu F. A strategy for improving mechanical properties of composite nanofibers through surface functionalization of fillers with hyperbranched polyglycerol. *J Mater Sci*. 2016;51(2):797–808.
49. Cai N, Dai Q, Wang Z, Luo X, Xue Y, Yu F. Toughening of electrospun poly(l-lactic acid) nanofiber scaffolds with unidirectionally aligned halloysite nanotubes. *J Mater Sci*. 2015;50(3):1435–1445.
50. Wang S, Li Y, Zhao R, Jin T, Zhang L, Li X. Chitosan surface modified electrospun poly(ε-caprolactone)/carbon nanotube composite fibers with enhanced mechanical, cell proliferation and antibacterial properties. *Int J Biol Macromol*. 2017;104(Pt A):708–715.
51. Schwartz R, Davidson T. Pharmacology, pharmacokinetics, and practical applications of bortezomib. *Oncology*. 2004;18(14 Suppl 11):14–21.
52. Unsoy G, Yalcin S, Khodadust R, Mutlu P, Onguru O, Gunduz U. Chitosan magnetic nanoparticles for pH responsive Bortezomib release in cancer therapy. *Biomed Pharmacother*. 2014;68(5):641–648.
53. Qu Y, Chu BY, Peng JR, et al. A biodegradable thermo-responsive hybrid hydrogel: therapeutic applications in preventing the post-operative recurrence of breast cancer. *NPG Asia Mater*. 2015;7(8):e207.
54. Zhang Z, Liu S, Xiong H, et al. Electrospun PLA/MWCNTs composite nanofibers for combined chemo- and photothermal therapy. *Acta Biomater*. 2015;26:115–123.
55. Strong LE, Dahotre SN, West JL. Hydrogel-nanoparticle composites for optically modulated cancer therapeutic delivery. *J Control Release*. 2014;178:63–68.
56. Li W, Wang J, Ren J, Qu X, Wen L, Jiasi W, Jinsong R, Xiaogang Q. 3D graphene oxide-polymer hydrogel: near-infrared light-triggered active scaffold for reversible cell capture and on-demand release. *Adv Mater*. 2013;25(46):6737–6743.
57. Chiang WL, Lin TT, Sureshbabu R, et al. A rapid drug release system with a NIR light-activated molecular switch for dual-modality photothermal/antibiotic treatments of subcutaneous abscesses. *J Control Release*. 2015;199:53–62.
58. Liu Y, Ashton JR, Moding EJ, et al. A Plasmonic Gold Nanostar Theranostic Probe for In Vivo Tumor Imaging and Photothermal Therapy. *Theranostics*. 2015;5(9):946–960.

Supplementary materials

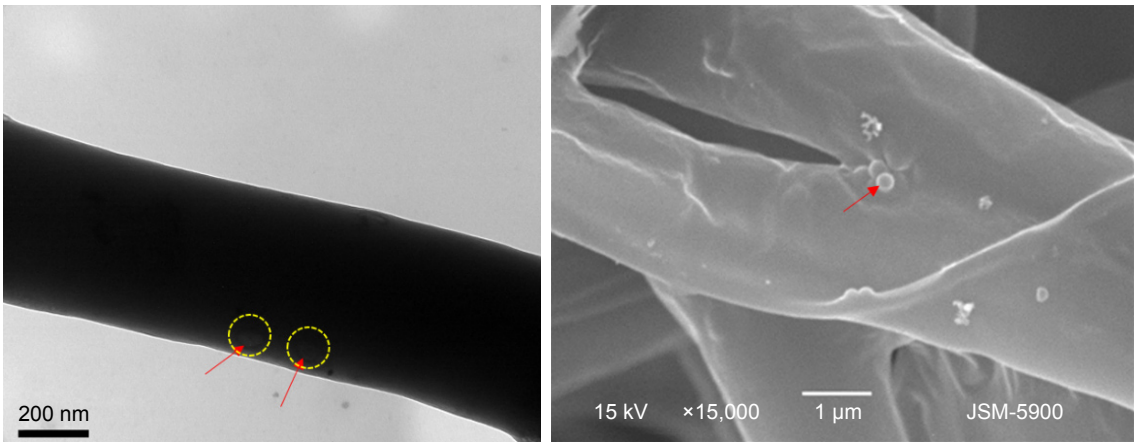

Figure S1 Bio-TEM (left) and SEM images (right) of PDO composite fiber with red arrow showing PD NPs closer to the fiber surface.
Abbreviations: Bio-TEM, bio-transmission electron microscopy; PD NPs, polydopamine nanospheres; PDO, polydioxanone; SEM, scanning electron microscopy.

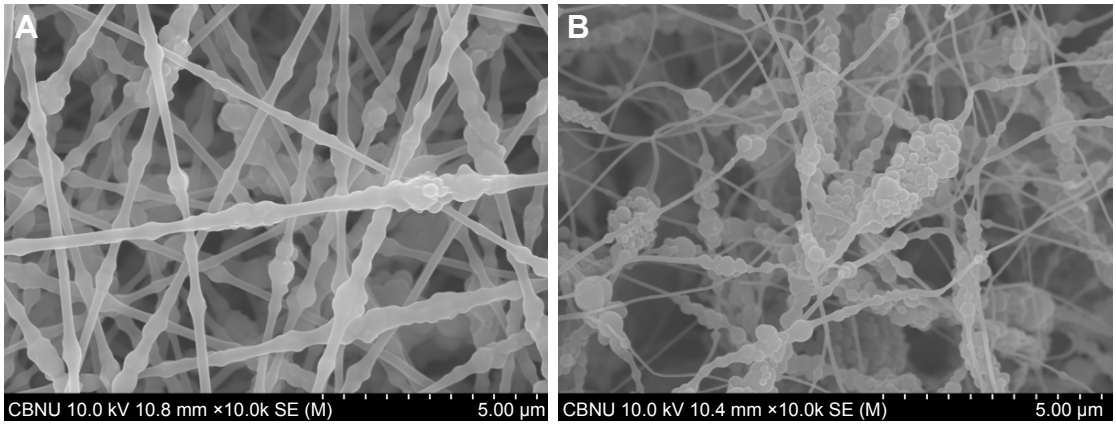

Figure S2 Morphology of PDO fiber incorporated with different concentration of PD NPs: (**A**) 5% and (**B**) 10%.
Abbreviations: PD NPs, polydopamine nanospheres; PDO, polydioxanone.

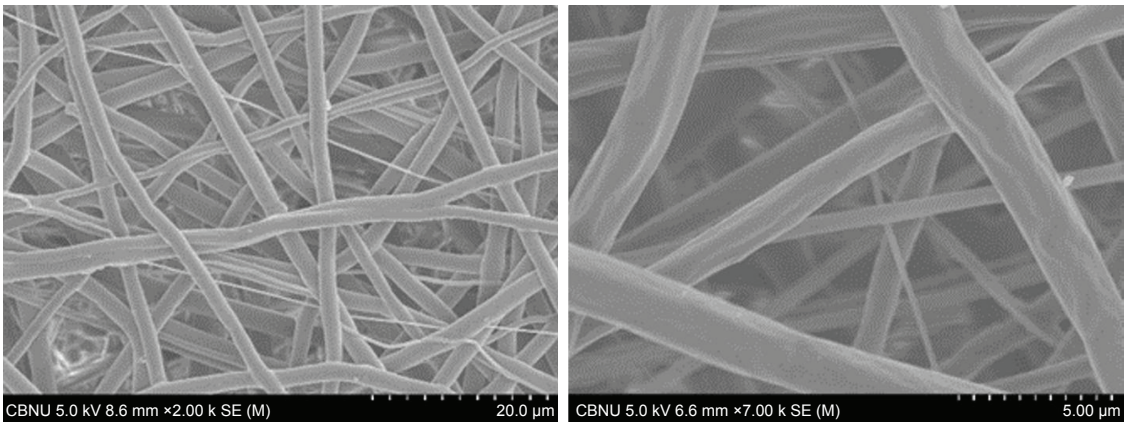

Figure S3 SEM image of neat PDO nanofiber after NIR irradiation (left, low magnification and right, high magnification).
Abbreviations: NIR, near-infrared; PDO, polydioxanone; SEM, scanning electron microscopy.

International Journal of Nanomedicine downloaded from https://www.dovepress.com/ by 43.243.61.32 on 17-Oct-2018
For personal use only.

International Journal of Nanomedicine downloaded from https://www.dovepress.com/ by 43.243.61.32 on 17-Oct-2018
For personal use only.

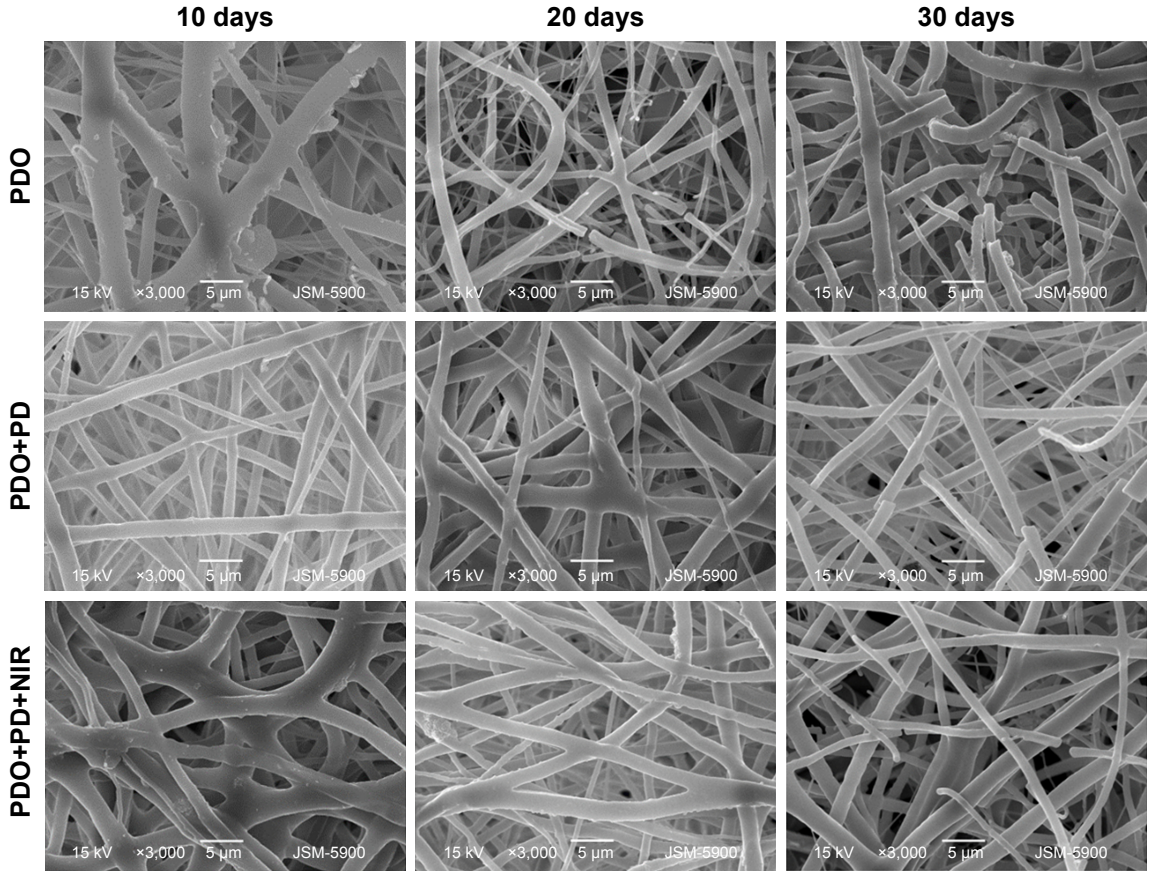

Figure S4 SEM microscopy of PDO, PDO+PD, and PDO+PD+NIR after 10, 20, and 30 days of degradation in vitro.
Abbreviations: NIR, near-infrared; PD, polydopamine; PDO, polydioxanone; SEM, scanning electron microscopy.

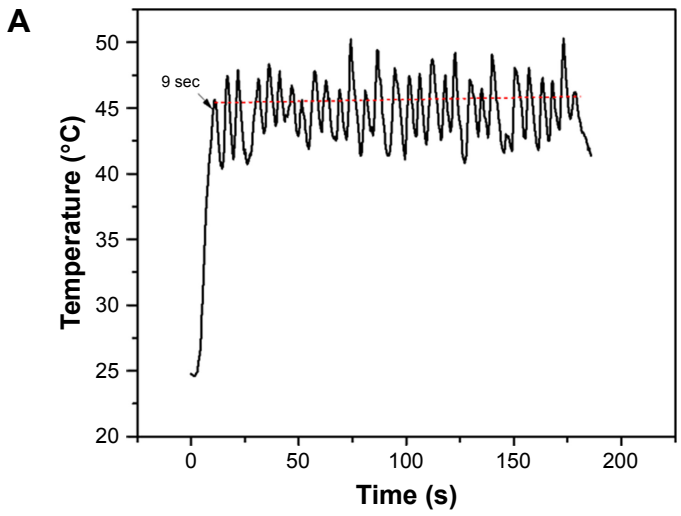

Figure S5 (*Continued*)

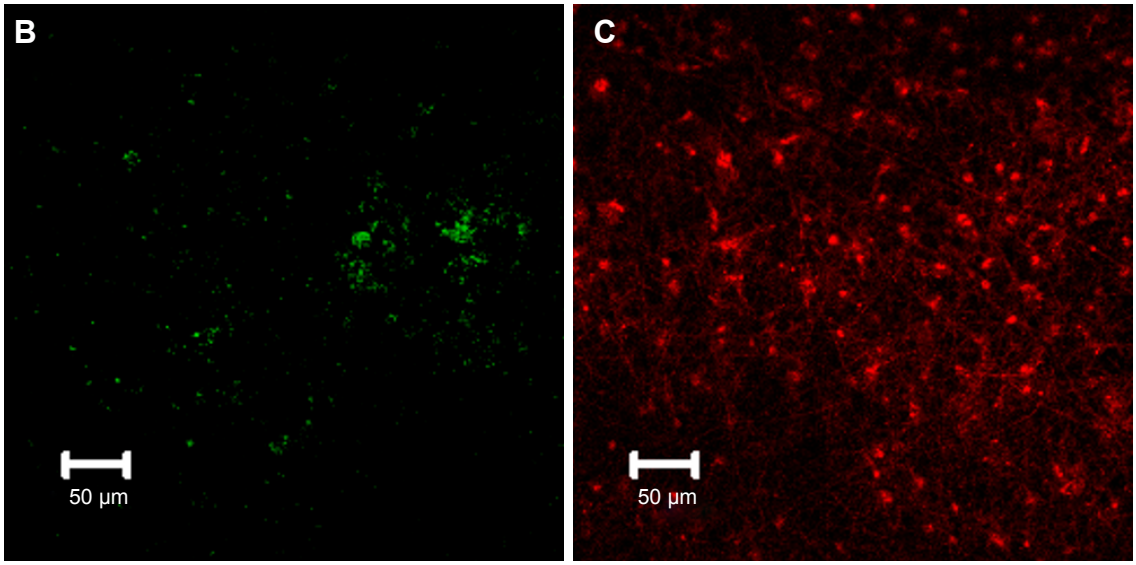

Figure S5 (**A**) Temperature profile for PDO+PD fiber with 808 nm, 2 W/cm^2 pulse laser of 1 second "off" and 2 seconds "on" after initial 9 seconds of continuous irradiation. (**B** and **C**) Combined photothermal and chemotherapy treatment for PDO+PD-BTZ nanofiber after 72 hours of treatment using control pulse laser after 3 minutes assessed by LIVE/DEAD® assay with CT26 cancer cells (green on the left is the remaining LIVE cells, whereas red on the right represent DEAD cells).
Abbreviations: PD, polydopamine; PDO, polydioxanone; BTZ, bortezomib.

Video abstract

Point your SmartPhone at the code above. If you have a QR code reader the video abstract will appear. Or use:

http://youtu.be/FgFWhuWCmv4

International Journal of Nanomedicine downloaded from https://www.dovepress.com/ by 43.243.61.32 on 17-Oct-2018
For personal use only.

International Journal of Nanomedicine

Dovepress

Publish your work in this journal

The International Journal of Nanomedicine is an international, peer-reviewed journal focusing on the application of nanotechnology in diagnostics, therapeutics, and drug delivery systems throughout the biomedical field. This journal is indexed on PubMed Central, MedLine, CAS, SciSearch®, Current Contents®/Clinical Medicine, Journal Citation Reports/Science Edition, EMBase, Scopus and the Elsevier Bibliographic databases. The manuscript management system is completely online and includes a very quick and fair peer-review system, which is all easy to use. Visit http://www.dovepress.com/testimonials.php to read real quotes from published authors.

Submit your manuscript here: http://www.dovepress.com/international-journal-of-nanomedicine-journal